Spirofluoreneacridinone-Based Shape-Controlled Nanorods for Aqueous Phase Processed Light-Emitting Devices Toward Green Organic Semiconductors and Electronics

Zong-Qiong Lin [†,§], Jin Liang [†,§], Su-Hui Yang [†,§], Huey Hoon Hng[‡], Ling-Hai Xie [†,§,*], Ming-Li Sun[†,§], Qi-Chun Zhang[‡], Hui-Ying Yang[‡], Wei Huang [†,§,*]

[†]Center for Molecular Systems and Organic Devices (CMSOD), Key Laboratory for Organic Electronics & Information Displays (KLOEID) and Institute of Advanced Materials (IAM), Nanjing University of Posts & Telecommunications, 9 Wenyuan Road, Nanjing 210046, China

[‡]School of Materials Science and Engineering, Nanyang Technological University, 50 Nanyang Avenue, Singapore 639798, Singapore;

[§]Jiangsu-Singapore Joint Research Center for Organic/Bio- Electronics & Information Displays and Institute of Advanced Materials, Nanjing University of Technology, Nanjing 211816, China.

[*]iamlhxie@njupt.edu.cn (L.-H. X.); iamwhuang@njupt.edu.cn (W.H.).

ABSTRACT

Aqueous phase processing of organic nanoscale semiconductors for organic light emitting diodes (OLEDs) are fascinating and become a hot topic owing to their merits of low-cost, greena and eco-friendly processing. Topological superiority of non-planar 3-dimensional molecules with supramolecular steric hindrance offers more degrees of freedom to design nonvcovalent driving forces to organize into nanostructures. We here demonstrate aqueous phase deposition of quasi-1D nanorod from the cruciform-shaped spiro[fluorene-9,7'-dibenzo[c,h]acridine]-5'-one (SFDBAO) into heterjunction thin-film LEDs. The length of as prepared SFDBAO nanorods undergo a kinetic morphology evolution from 2.12 to 11.09 μm, with an elongated octahedron at the edge. A well n-type semiconducting property is investigated with a broad EL emission at ~ 600 nm, through the as prepared LED.

Keywords: Organic nanorods, aqueous processing, spiro compounds, thin films, self-assembly, organic light-emitting devices

1 INTRODUCTION

Synthesis of large-area and high-quality thin fims via aqueous phase fabrication and deposition technique are attracting a growing interests in organic optoelectronic devices owing to green, eco-friendly, and sustainable advantages over oraganic solution processing.[1-3] Although aqueous processed thin films of conjugated polymers has been realized through the introduction of water soluble side groups, it requires laborious organic synthesis and suffer from the complicated purification.[4-6] Nano-engineering offer an prospective and convenient alternative to aqueous suspensions and inks containing semiconducting organic nanostructure for the fabrication of the nanostuctured thin-films toward green and sustainable organic devices.

The most reported examples are the 0D amorphous conjuated polymer nanoparticles or nanospheres for the application in polymer light emitting diodes (PLEDs). Aqueous polyethylene dioxythiophene: polystyrene sulfonate (PEDOT: PSS) suspensions [7, 8] has been extensively applied as the hole transport and electron blocking layer. Aqueous processed conjugated polymer nanoparticles have acted as the active light-emitting layers in PLEDs [9-11]. For the 1D nanomaterial, a low degree of crystallinity poly(9,9-dioctylfluorene) nanowire [12] has been introduced into blue light emitting electrochemical cells from its aqueous suspension. However, there are very rare concerns about the nanoengineering of low-molecular-weight organic semiconductors (LMWOSs) for organic light-emiting devices (OLEDs). Zhang and Yang et al., actualized the heterojunction LEDs from crystalline coronene, aroyleneimidazophenazine nanowires [13, 14] and 9,10-diphenylanthracene nanorods, [15] whose electroluminescence (EL) display the appealing morphology dependence. Nevertheless, efforts still should be made to explore organic semiconducting nanostructures, their aqueous suspensions and inks as well as nanostructured thin films in the framework of green organic electronics or optoelectronics.

Over the past decades, dynamic surface solvation (selective adhesion) provides a versatile approach to kinetically control over crystal growth in the 1D inorganic counterpart.[16] However, bottom-up synthesis of kinetic shape-controlled 1D nanostructures from LMWOSs is proposed as a thorny challenge, [17, 18] due to the rather weak supramolecular interactions, making kinetic growth mechanisms complicated and the unclear correlation between crystal morphology and molecular configuration. Topological superiority of non-planar 3D configuration offers more degrees of freedom to design various organic nanostructures. We create cruciform-shaped spirocyclic aromatic hydrocarbons (SAHs) as the state-of-the-art models of 3-dimensional molecules with supramolecular steric hindrance are promising versatile molecular building blocks for self-assembly.[19] In previous works, the highly symmetric polyhedral nanocrystals from spiro[fluorene-

9,7'-dibenzo[c,h]acridine]-5'-one (SFDBAO) have been well grown by syngertic compitition between internal driving forces such as steric hindrance-induced π-π stacking aromatic planes and external confined interactions such as between crystal facets and surfactents.[19] Herein, we demonstrated the aqueous processing of a heterojunction OLED from SFDBAO quasi-1D nanorods, whose shape and length can be tailored by kinetic morphology evolution of self-assembly.

2 RESULT AND DISSCUSSION

2.1 SFDBAO Packing Motifs

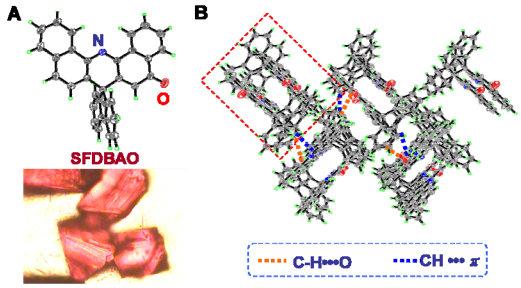

Figure 1. (A) Single molecular configuration of SFDBAO from its crystallographic data. The inset of A: the photograph of SFDBAO single crystal in octahedron. (B) Packing motifs of SFDBAO crystal, with C−H•••π, C−H•••O hydrogen bonding.

The modeling compound SFDBAO was synthesis via a concise eco-friendly visible-light-mediated photooxygenation with auto-catalyzed and self-sensitive mechanisms according to the previous procedure. [19] A series of polyhedra, ranging from octahedron, elongated octahedron, hexahedron, decahedron, to elongated decahedron, have been obtained previously, by manipulating the kinetic self-assembly. Figure 1A schemes out the single molecular configuration of SFDBAO from its crystallographic data. The orthorhombic SFDBAO belongs to the space group symmetry of P_{212121} (19), with cell parameters of a = 11.260(2) Å, b = 12.060(2) Å, c = 16.530(3) Å, a/b=0.9337 b/c=0.7296 c/a=1.4680. The photograph of the red SFDBAO single crystal was shown in octahedron (inset of Figure 1A). Figure 1B illustrated vertical molecular packing motifs among SFDBAO through the supramolecular C−H•••π, C−H•••O hydrogen bonding and π•••π stacking interactions that were observed along the {020}s direction. The details of weak interactions in the molecular packing are illustrated in a dimmer of SFDBAO (dash red-circle), with the π•••π stacking between acridine and naphthalene moieties (as the distance of 3.56 Å) via C−H•••O (2.32 Å) and C−H•••π (2.33 Å) noncovalent interactions. Subsequent of the dimmers can be dominated and integrated by C−H•••O (2.71 Å) and C−H•••π (2.68 Å) interactions as dash line remarked. From the molecular packing analysis, the essential reason for resulting polyhedral morphology was attributed to its 3D geometric shapes that induce mulitple and multiscale interactions in framework of the time-space. This result indicated topology design of 3-dimensional molecules are key point to deeply get insight into the shape relations between molecules and nanostuctures. By means of kinetic self-assembly that is another factor to further tailor the morphology by tuning the cohesive energies of crystal facets with the assistance of surfactants, it is predicted that the quasi-1D nanorods of SFDBAO can be obtained.

2.2 Shape-controlled Synthesis of SFDBAO Nanorods

The aqueous suspension of quasi-1D nanorod from SFDBAO was prepared via a classical reprecipitation method with the assistance of Pluronic 123 (P123). A series volume of SFDBAO/ tetrahydrofuran (THF) storage solution in different concentration, 1 mL (1 mM), 0.75 mL (1.33 mM, recorded as A), 0.5 mL (2 mM) and 0.25 mL (4 mM, recorded as B) was injected into 5 mL P123 aqueous solution (1 mg/mL). After stirring for 5 min, the sample was maintained at room temperatures (20 °C) for about 48 hours to stabilize the nanostructures. The samples suffered subsequently from separation via decanting the supernatant liquid after centrifugation and washed with pure water for 3 times.

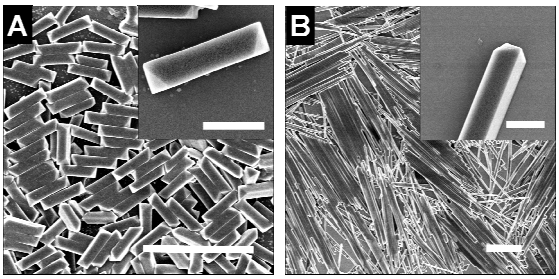

Figure 2. SEM images of SFDBAO nanorod A and B, with the length of 2.12 (A) and 11.09 μm (B), respectively. The scale bar is 5 μm. The inset: the enlarged morphology of nanorod A and edge of nanorod B (the scale bar is 1 μm).

Noted that, the length of SFDBAO nanorods was measured as 0.89 (see ref. 19), 2.12, 5.19 (support information) and 11.09 μm for 1, 0.75, 0.5, 0.25 mL, respectively. Typical scan electron microscopy (SEM) images of the nanorod A and B were shown in Figure 2 with uniform morphology and sizes. Nanorod A (Figure 2A) exhibits a remarkable larger respect ratio compared with the elongated octahedron in ref. 19. The inset of A gave out the single nanorod A with clean crystal facets. The self-organized bundles of nanorod B even observed when dropcasting such rigid nanostructure on silicon substrate (Figure 2B). The nanorod B presents a well defined octahedron at the edge, which suggested the kinetic growth along {002}s directions from 3D polyhedron. The essential reason for such shape-controlled process is attribute to the increase of surface energy by reduced change the volume ratio of THF/water during self-assembly.

2.3 XRD characterization and Optical Properties

In order to further get inside into the kinetic growth of SFDBAO nanorod, the powder X-ray diffraction (XRD)

was performed. Both of the nanorod A and B are suffered an identical well-defined XRD profiles (Figure 3A), indicating the excellent crystallization. We can figure out that the *d* spacing values at 9.49, 8.71, 7.41, 4.74 and 3.71 Å of diffraction peaks are assigned as {101}s, {002}s, {111}s and {202}s, respectively, according to the crystallographic data. As the comparison of nanorod A (blue line) and B (wine line), the much stronger diffraction intensity in {002}s of B was observed that was considered as further evidence on latitude growth of nanorods.

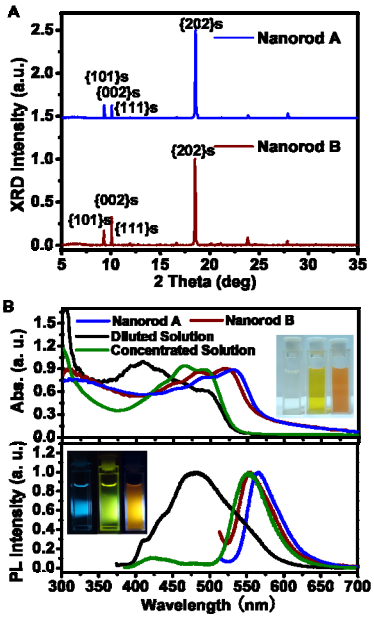

Figure 3. Powder XRD (A), UV-vis absorption and fluorescence spectra (B) for the nanorod A (blue line), B (wine line) and THF solution (black line). The photogaraphe of SFDBAO THF diluted solution (left), concentrated solution (middle), nanorod (right) in the day light (inset of A) and the visual fluorescent color (inset of B) under the 365 nm UV lamp.

SFDBAO and its nanorod suspensions exhibit abundant spectra behaviors. The UV-vis absorption and fluorescence spectra of SFDBAO polyhedra are shown in Figure 3B. In its THF diluted solution (1×10^{-5} M), the absorbance λ_{max} located at ~ 495 nm, which may be attribute to the n-π* transition of SFDBAO. It suffered a remarkable concentration dependents on the absorbance behavior, whose absorption band was enhanced at 464~490 nm in its high concentrated solution (1×10^{-3} M). An obvious red-shift of 20~30 nm was observed, when examining the SFDBAO nanorod aqueous suspension (at 520~530 nm), compared with that of solution. The baseline drift may attribute to the scattering of nanorod. As revealed by the photographs in the inset of Figure 3A, a colorless, bright yellow and orange of SFDBAO solution (or suspension) was present as THF diluted solution (left), concentrated solution (middle), nanorod (right), respectively. The broad emission band of its diluted solution from 400 ~ 600 nm (482 nm as the peak position) was distinct from the concentrated solution, whose profile was divided into two parts as 400 ~ 450 and 520~600 nm (with the peak position at 551 nm). Moreover, the nanorods emitted a sharp orange color with a 3~18 nm red-shift (at ~560 nm) instead of its THF solution. Noted that, the nanorod B possesses a length dependence of spectra behavior whose broad absorbance band was located at 520 nm (10 nm blue-shift), as well as the a blue shift of 15 nm *vs*. nanorod A. Both of the concentration and length dependence may attribute to the J-aggregate and charge transfer between the stacked acridnes and naphthalene moieties according to SFDBAO crystallographic data. The inset of Figure 3B illustrated the photographs of blue emission of SFDBAO in THF diluted solution (left), green emission in concentrated solution (middle), and orange emission in nanorod (right) under the 365 nm UV lamp.

2.4 OLED by Aqueous Phase Processing and Evaluation

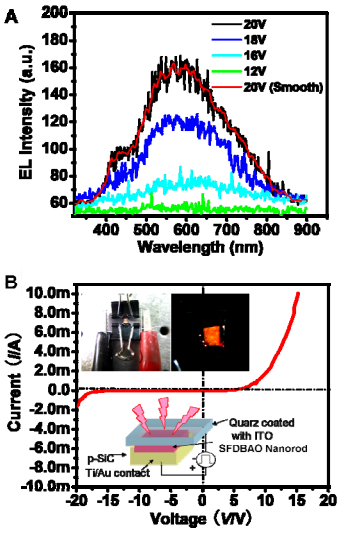

Figure 4. EL spectra (A) and current-voltage (I-V) curve (B) of the p-SiC/SFDBAO nanorod/ITO heterojunction OLED. Inset of B shows the scheme and photographs of the heterojunction OLED.

Our aims to investigate semiconducting properties of SFDBAO nanorods, a prototype OLED was fabricated by aqueous processing with a sandwich-like device structure of p-SiC/SFDBAO nanorod/ITO (as schemed in the inset of Figure 4) [20]. Nanorod thin films using the active light-emiting layers was deposited by drop casting aqueous suspensions with volume of ~50 μL onto *p*-type 4H–SiC substrate. Figure 4A reveals the EL spectra of the LED, when a forward bias voltage of 12, 16, 18 and 20 V was applied. A broad emission band at ~ 600 nm (as smoothing the PL curve at 20 V) was displayed a remarkable intensity increase with a larger positive bias. By contrast, no light emission was observed from the heterojunction LED under reverse bias. The insets of Figure 4B show the photographs in fabrication of a LED (left) and its EL emission (right) in the dark. Figure 4B plots the current-voltage (I-V, in red) curve of the heterojunction at ambient atmosphere. It is observed that the heterojunction has a turn-on voltage of ~

6 V, nevertheless, its EL spectra won't be obtained until 12 V. The rectifying diode behavior of OLED with a low leakage current under reverse bias indicates an n-type electron injecting properties of the SFDBAO nanorod in the heterojunction devices.

3 CONCLUSIONS

In summary, non-planar 3D cruciform-shaped SFDBAO with supramolecualr steric hindrance self-assembled into a series of length-controlled nanorods with an excellent crystallization through kinetically controlled growth. UV-vis and PL spectra in nanorods exhibited obvious length dependent features. Aqueous processed thin film OLEDs with the configuration of p-SiC/SFDBAO nanorod/ITO displayed the rectifying behaviors and the red emission color with a broad peak at ~ 600 nm. Aqueous organic nanostructures will be potenial organic nano inks for the fabrication of nanostructured thin films toward green and eco-friendly organic electronics, which are also compatible with cost-effective roll-to-roll and inkjet printing technique in printed and flexible electronics. Organic nano-engineering provides another facile approach to fabricate green organic devices.

EXPERIMENT

Method: For SEM studies, a drop of 20 μL nanorod was placed onto silicon substrate, and the solvent was left to evaporate. The samples were then examined with a field emission SEM (Hitachi, S-4800) at an accelerating voltage of 5 kV. The XRD patterns were performed on a Bruker D8 X-ray diffractometer with Cu Kα radiation (λ = 1.54050 Å). The operating 2θ angle ranged from 5 to 70°, with the step length of 0.025°. *Device fabrication*: The contact of the heterojunction was fabricated by depositing a metal layer of dimension about 2×2 mm^2, which consisted of a layer of ~ 25 nm thick Al film and a layer of ~ 150 nm thick Ti film, onto the rough surface of the p-SiC substrates via electron beam evaporation. The sample was then subjected to rapid thermal annealing at 800 °C in N2 for 5 min in order to obtain an Ohmic contact on the p-SiC substrate, the corresponding contact resistance was less than 2 kΩ. A drop of polyhedra (~ 50 μL) was placed onto the substrates, and left to evaporate. A constant voltage was applied on the sample for all EL measurements, and the EL signal was detected by a photomultiplier detector connected with a monochromator and collected from an optical fiber.

ACKNOWLEDGMENT

The authors acknowledge financial support from National Basic Research Program of China (973 Program, 2009CB930601), National Natural Science Foundation of China (21274064, BZ2010043, 20974046, 20774043, 51173081, 50428303, 61136003, 21144004, 51273092, 61106058), the Program for New Century Excellent Talents in University (NCET-11-0992), Natural Science Foundation of Jiangsu Province (BK2011761, BK2008053, BK2009025, 10KJB510013), Funding of Jiangsu Innovation Program for Graduate Education (CXZZ11_0413). X. L. H. thanks Jiangsu Overseas Research & Training Program for University Prominent Young & Middle-aged Teachers and Presidents.

REFERENCES

[1] T. Kietzke, D. Neher, K. Landfester, R. Montenegro, R. Guntner and U. Scherf, *Nat. Mater.,* 408-412, **2**, 2003.

[2] T. R. Andersen, T. T. Larsen-Olsen, B. Andreasen, A. P. L. BÖttiger, J. E. Carlé, M. Helgesen, E. Bundgaard, K. Norrman, J. W. Andreasen, M. Jørgensen and F. C. Krebs, *ACS Nano*, 4188-4196, **5**, 2011.

[3] R. Søndergaard, M. Helgesen, M. Jørgensen and F. C. Krebs, *Adv. Energy Mater.,* 68-71, **1**, 2011.

[4] F. Huang, H. Wu and Y. Cao, *Chem. Soc. Rev.,* 2500-2521, **39**, 2010.

[5] R. Yang, Y. Xu, X.-D. Dang, T.-Q. Nguyen, Y. Cao and G. C. Bazan, *J. Am. Chem. Soc.*, 3282-3283, **130**, 2008.

[6] C. Duan, C. Zhong, C. Liu, F. Huang and Y. Cao, *Chem. Mater.,* 1682-1689, **24**, 2012.

[7] M. Brun, R. Demadrille, P. Rannou, A. Pron, J. P. Travers and B. Grévin, *Adv. Mater.*, 2087-2092, **16**, 2004.

[8] S. K. M. Jonsson, J. Birgerson, X. Crispin, G. Greczynski, W. Osikowicz, A. W. Denier van der Gon, W. R. Salaneck and M. Fahlman, *Synth. Met.*, 1-10, **139**, 2003.

[9] T. Piok, S. Gamerith, C. Gadermaier, H. Plank, F. P. Wenzl, S. Patil, R. Montenegro, T. Kietzke, D. Neher, U. Scherf, K. Landfester and E. J. W. List, *Adv. Mater.*, 800-804, **15**, 2003.

[10] E.-J. Park, T. Erdem, V. Ibrahimova, S. Nizamoglu, H. V. Demir and D. Tuncel, *ACS Nano*, 2483-2492, **5**, 2011.

[11] C. F. Huebner, R. D. Roeder and S. H. Foulger, *Adv. Funct. Mater.*, 3604-3609, **19**, 2009.

[12] D. O'Carroll, D. Iacopino, A. O'Riordan, P. Lovera, É. O'Connor, G. A. O'Brien and G. Redmond, *Adv. Mater.*, 42-48, **20**, 2008.

[13] J. Xiao, H. Yang, Z. Yin, J. Guo, F. Boey, H. Zhang and Q. Zhang, *J. Mater. Chem.,*1423-1427, **21**, 2010.

[14] J. Zhao, J. I. Wong, C. Wang, J. Gao, V. Z. Y. Ng, H. Y. Yang, S. C. J. Loo and Q. Zhang, *Chem. Asian J.,* 665-669, **8**, 2013.

[15] B. Yang, J. Xiao, J. I. Wong, J. Guo, Y. Wu, L. Ong, L. L. Lao, F. Boey, H. Zhang, H. Y. Yang and Q. Zhang, *J. Phys. Chem. C,* 7924-7927, **115,** 2011.

[16] Y. Yin and A. P. Alivisatos, *Nature*, 664-670, **437**, 2005.

[17] Y. S. Zhao, H. Fu, A. Peng, Y. Ma, D. Xiao and J. Yao, *Adv. Mater.*, 2859-2876, **20**, 2008.

[18] J. Xiao, Z. Yin, H. Li, Q. Zhang, F. Boey, H. Zhang and Q. Zhang, *J. Am. Chem. Soc.*, 6926-6928, **132**, 2010.

[19] Z.-Q. Lin, P.-J. Sun, Y.-Y. Tay, J. Liang, Y. Liu, N.-E. Shi, L.-H. Xie, M.-D. Yi, Y. Qian, Q.-L. Fan, H. Zhang, H. H. Hng, J. Ma, Q. Zhang and W. Huang, *ACS Nano*, 5309-5319, **6**, 2012.

[20] H. Y. Yang, S. F. Yu, Y. Y. Hui and S. P. Lau, *Appl. Phys. Lett.,* 191105-191103, **97**, 2010.